Iranian Society of Acoustics and Vibration
Iranian Society of
Acoustics and Vibration
The 15th ISAV2025
International Conference on
Acoustics and Vibration
24-25 Dec 2025 Tehran- Iran

Design of electro-acoustic Tonpilz transducer for underwater SONAR applications with Finite Element Method

Mohammad Amiri [a*], Saeid Sefidgar [a], Amir Kabiri [a], Saber Soltanrezaei [a],
Sajad Ghajarpoor [b], Sedigheh Shekarriz Lari [c]

[a] *Researcher, Acoustic and Sonar Center, Research Organization, Tehran, Iran.*

[b] *Researcher, Department of Physics, Shiraz University of Technology, Shiraz, Iran.*

[c] *PhD Candidate, Department of Physics, Shiraz University, Shiraz, Iran.*

** Corresponding author e-mail: Amiri.s.1373@gmail.com*

Abstract

This study aims to design and fabricate an acoustic transducer whose first resonance frequency occurs within the 11 kHz range. The transducer can be used as an underwater warning pinger (locator) for emergency situations. When installed on an aircraft, vessel, or piece of equipment, and activated by a pressure sensor, this pinger can serve as a warning device. The core of the transducer is a piezoelectric (PZT-4) ring. By adding a concentric cylindrical metal shell around the ring, we aim to both increase the structural degrees of freedom and align the emitted acoustic wave with the normal vector perpendicular to the outer surface of the ring. The ring is made of piezoceramic material, while the surrounding concentric metal shell is made of aluminum. Since the computational analysis of such structures using simulation software is highly time-consuming, a sector of the structure is analyzed instead of the full model, as the results are identical to those obtained from the complete geometry. The obtained results show excellent agreement.

Keywords: Tonpilz; transducer; FEM.

---

1. Introduction

The Pinpointing System, or Underwater Backscatter Localization (UBL), is a novel underwater navigation technology. Unlike conventional positioning systems such as GPS, which rely on radio waves, UBL operates using acoustic signals, since radio waves rapidly attenuate and lose strength in liquids particularly in seawater [1,2].

In underwater environments, researchers rely on acoustic methods to track various objects and marine species such as unmanned submarines, whales, and schools of fish, as well as to monitor underwater acoustic signaling. The UBL system generates binary pulses through the backscattering of acoustic signals and utilizes them for precise localization. The ultimate goal of this technology is to develop an efficient navigation system capable of producing accurate and wide-area maps of the oceans [3-7].

As such technologies advance, the deployment of unmanned underwater vehicles (UUVs) in deep-sea environments will become increasingly feasible. Positioning and navigation systems play a vital role in both industrial and scientific operations; without them, many underwater missions would be extremely difficult or even impossible to accomplish. While GPS is highly effective for land and aerial applications, it cannot function underwater, as water blocks the propagation of radio waves. Consequently, submarines use sonar instead of radar, since acoustic signals can propagate for thousands of kilometers under favorable conditions [8-12].

According to researchers at MIT, one of the primary challenges in using acoustic systems for underwater localization is their high energy consumption. Large submarines can easily provide sufficient power for their acoustic systems; however, smaller devices designed for applications such as marine animal tracking are limited by power availability and the need for large batteries [13-15].

To address this issue, researchers have employed piezoelectric materials. In the UBL system, piezoelectric sensors harvest energy from reflected acoustic waves in the surrounding environment. These sensors selectively capture returning signals and convert them into a power source for the device [16-20].

Several experiments have been conducted on the UBL system, and the results demonstrate promising performance in shallow-water environments, marking a significant step toward the realization of low-power, battery-free underwater navigation technologies [21-27].

2. Tonpilz transducer

Underwater acoustics has emerged as a critical field of research due to its extensive range of scientific and industrial applications, including sonar systems, underwater communication, and marine environmental monitoring. In this context, arrays of electroacoustic transducers are widely employed as both transmitters and receivers of acoustic waves in underwater environments. Among various types of underwater transducers, the Tonpilz transducer is the most prevalent due to its high efficiency and structural simplicity. Fig. 2 presents a cross-sectional schematic of a Tonpilz transducer along with several representative examples.

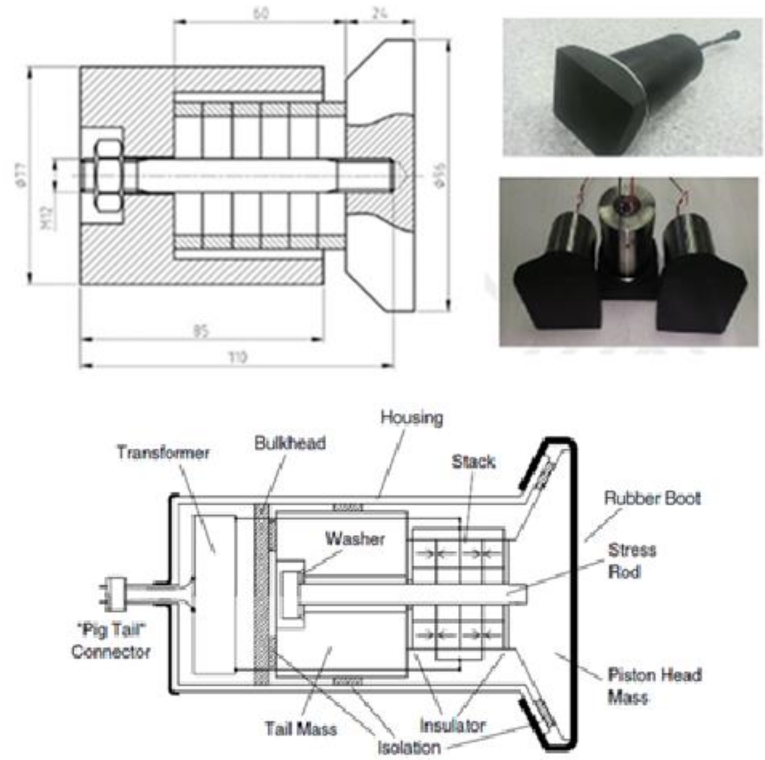

Figure 2: Left: Cutaway view of a Tonpilz Transducer and right: Full view of a Tonpilz Transducer after insulation [30].

A conventional Tonpilz transducer is composed of four primary components: a head mass, a tail mass, a stack of piezoelectric ceramic rings or disks, and a pre-stressing bolt. Depending on specific design requirements, additional elements such as metal electrodes, adhesive layers, rubber insulators, and other auxiliary materials may also be incorporated into the structure.

The assembly process typically begins with the concentric stacking of multiple piezoceramic rings. Depending on the electrical configuration, metal electrodes or intermediate conductive layers are inserted between the ceramics. Subsequently, the head and tail masses are positioned at the upper and lower ends of the stack, respectively, and the entire assembly is clamped together using a central bolt. The bolt penetrates approximately halfway into the head mass and is tightened on the tail side with a nut to ensure the required pre-stress and mechanical stability.

Several methodologies have been developed for the design and analysis of Tonpilz transducers, which are generally categorized into two main groups: analytical methods and numerical techniques. In a typical design workflow, the preliminary design stage employs simplified one-dimensional analytical models to obtain approximate dimensions of the transducer's key components based on target specifications such as resonance frequency and operational bandwidth.

In the commonly adopted lumped-parameter model, the Tonpilz transducer is represented as a mass spring mechanical system (Fig. 3). Using classical vibration equations and the prescribed resonance frequency, the approximate dimensions and mass distribution of the transducer components can be determined. An alternative one-dimensional representation is the equivalent electrical circuit model (Fig. 4), which exhibits strong analogy with the lumped-parameter model but utilizes electrical circuit elements and network laws to characterize the dynamic behavior of the transducer system.

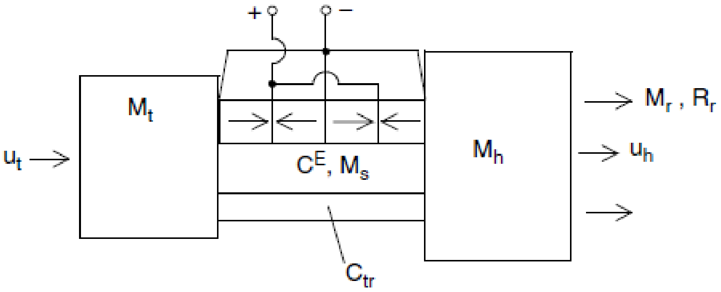

Figure 3: Initial mechanical model [31].

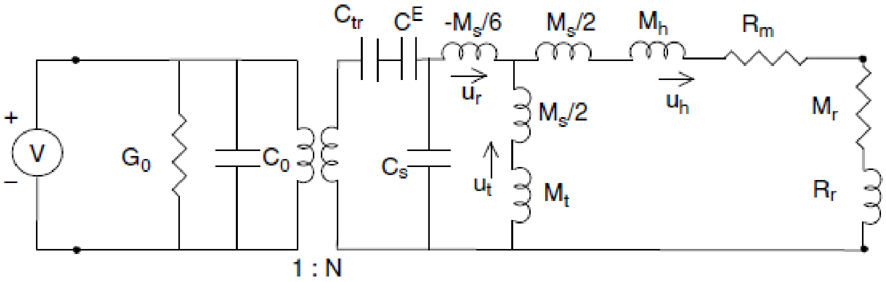

Figure 4: Analog circuit model for a Tonpilz transducer [32].

2.1 Technical Specifications and Discussion

Based on preliminary studies and design recommendations, the PZT-4 piezoceramic element was selected as the active material for the proposed transducer. Accordingly, the design aimed to develop a structural configuration capable of meeting the operational and mechanical requirements of the intended application.

To generate acoustic waves at the desired operating frequency, a set of piezoceramic components was employed. The proposed design was developed considering the available piezoceramic elements and their electromechanical properties. The selection of the transducer housing materials was made in accordance with conventional and experimentally validated designs. Using the data summarized in the following tables, the most suitable materials and their physical characteristics were determined.

Table 2: Materials used in the structure of Tonpilz [33-34].

head mass	Tail mass	bolt
Aluminum	steel	steel
Aluminum 6061	steel	steel
Aluminum	brass	Alloy steel
Aluminum	steel	Alloy steel

Table 3: Specifications of various types of PZT piezoceramics.

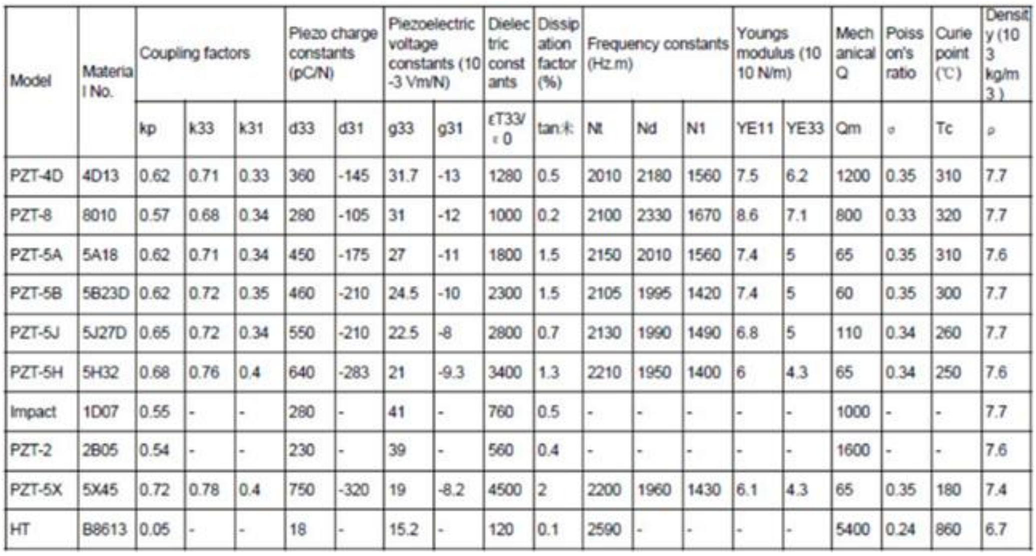

Model	Material No.	Coupling factors			Piezo charge constants (pC/N)		Piezoelectric voltage constants (10 -3 Vm/N)		Dielectric constants	Dissipation factor (%)	Frequency constants (Hz.m)			Youngs modulus (10 10 N/m)		Mechanical Q	Poisson's ratio	Curie point (℃)	Density (10 3 kg/m 3)
		kp	k33	k31	d33	d31	g33	g31	εT33/ε0	tan水	Nt	Nd	N1	YE11	YE33	Qm	σ	Tc	ρ
PZT-4D	4D13	0.62	0.71	0.33	360	-145	31.7	-13	1280	0.5	2010	2180	1560	7.5	6.2	1200	0.35	310	7.7
PZT-8	8010	0.57	0.68	0.34	280	-105	31	-12	1000	0.2	2100	2330	1670	8.6	7.1	800	0.33	320	7.7
PZT-5A	5A18	0.62	0.71	0.34	450	-175	27	-11	1800	1.5	2150	2010	1560	7.4	5	65	0.35	310	7.6
PZT-5B	5B23D	0.62	0.72	0.35	460	-210	24.5	-10	2300	1.5	2105	1995	1420	7.4	5	60	0.35	300	7.7
PZT-5J	5J27D	0.65	0.72	0.34	550	-210	22.5	-8	2800	0.7	2130	1990	1490	6.8	5	110	0.34	260	7.7
PZT-5H	5H32	0.68	0.76	0.4	640	-283	21	-9.3	3400	1.3	2210	1950	1400	6	4.3	65	0.34	250	7.6
Impact	1D07	0.55	-	-	280	-	41	-	760	0.5	-	-	-	-	-	1000	-	-	7.7
PZT-2	2B05	0.54	-	-	230	-	39	-	560	0.4	-	-	-	-	-	1600	-	-	7.6
PZT-5X	5X45	0.72	0.78	0.4	750	-320	19	-8.2	4500	2	2200	1960	1430	6.1	4.3	65	0.35	180	7.4
HT	B8613	0.05	-	-	18	-	15.2	-	120	0.1	2590	-	-	-	-	5400	0.24	860	6.7

Consequently, Aluminum was selected for the head mass, while stainless steel with an appropriate hardness level was used for the tail mass (body). The components were mechanically joined using a stainless-steel bolt, ensuring both rigidity and corrosion resistance. In several regions, rubber washers and insulating layers were inserted to prevent direct contact between the piezoceramic elements and the metallic housing. Moreover, waterproof insulating coatings were applied to the transducer's external surface to protect the internal structure from water ingress.

The following section presents the detailed technical specifications, final design parameters, and analytical results of the developed Tonpilz transducer.

2.2 Analysis of Stress Distribution in Tonpilz Transducers

As illustrated in Fig. 5, the investigation of vibration modes at various operating frequencies provides valuable insight into the stress distribution within the Tonpilz transducer structure. The variation of stress levels with increasing frequency reveals the underlying mechanical behavior of the transducer and validates the rationale behind its distinctive design configuration.

The mushroom-shaped design of the Tonpilz transducer, combined with the use of a lightweight metal such as aluminum for the head mass, leads to a localized increase in stress concentration at the head region. This stress concentration enhances the transmission of vibrational energy through the structure, thereby improving the efficiency of acoustic wave radiation into the surrounding medium.

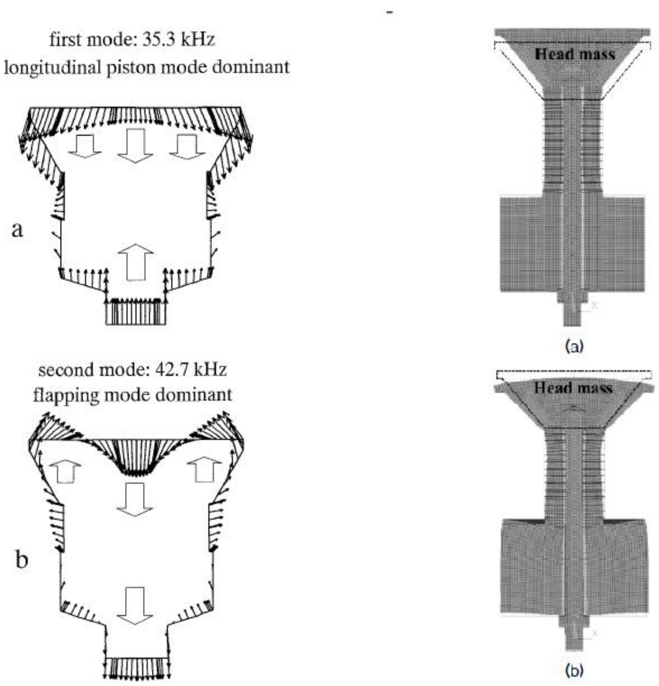

Figure 5: Stress distribution on the head mass of the Tonpilz transducer.

3. Experimental Conditions and Transducer Placement

The experiment was conducted in a controlled pool environment, with the transducer positioned at a short distance from the receiving hydrophone. The electrical circuitry and driving electronics were connected to the transducer, which was then submerged in water to generate acoustic ping signals for performance evaluation. All measured data were recorded and analyzed to assess the transducer’s acoustic and electrical behavior. The final performance results were determined following the completion of the experimental tests.

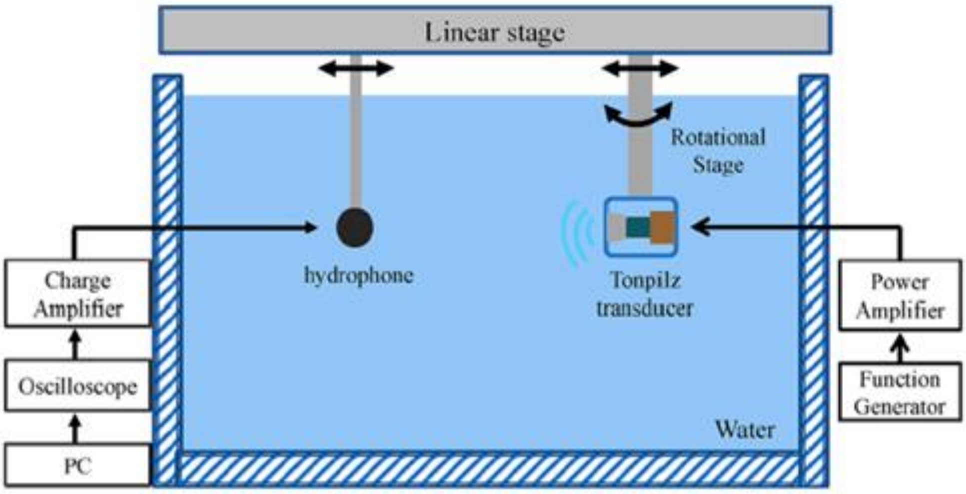

Figure 6. Schematic diagram showing the placement of the fabricated Tonpilz transducer in water for measuring the Transmitting Voltage Response (TVR).

4. Simulation and Modeling

This section presents the simulation and modeling process of the piezoceramic components, including both ring and disk structures, within the desired frequency range. Initially, individual piezoceramic elements were simulated to obtain their directivity patterns and stress distribution profiles under different excitation frequencies.

Subsequently, a complete model of the Tonpilz transducer was developed in a simulated underwater environment, allowing for the analysis of frequency response, acoustic radiation characteristics, and mechanical stress behavior at resonance frequencies. Several design variations using different materials and geometric configurations were evaluated to identify the optimal structure for maximum acoustic efficiency.

4.1 Single-Element Simulation

To design the pinger transducer, a PZT-4 piezoceramic ring with an inner radius of 15 mm, outer radius of 30 mm, and height of 10 mm was modeled. Fig. 7 presents the frequency–impedance curve and the 3D stress distribution at the resonance frequency of the piezoceramic. The dimensions of the element were selected based on availability and ease of access.

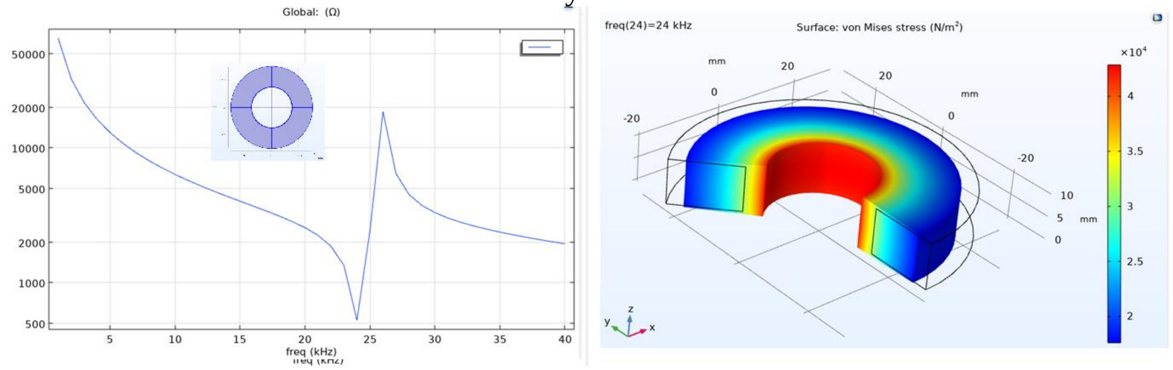

Figure 7: Piezoceramic ring — (left) frequency–impedance plot (resonance frequency: 24 kHz); (right) 3D stress distribution at resonance.

The pinger transducer consists of piezoceramic, head, tail, and bolt components. In this design, four PZT-4 piezoceramic rings were used, resulting in improved performance compared to conventional models. The use of four rings enhances the operational frequency and overall efficiency of the transducer. Fig. 8 shows the sectional view and 2D CAD drawing of the transducer design. In the design of this pinger, aluminum alloy 6061 was used for the head and housing components, while stainless-steel 316 was employed for the tail and bolt to ensure high mechanical strength and corrosion resistance in the underwater environment.

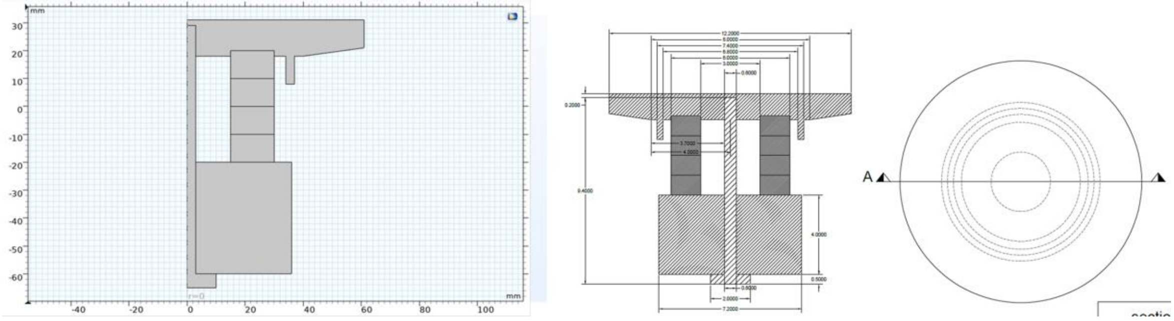

Figure 8: (a) Sectional view of the transducer including piezoceramic, head, tail, and bolt; (b) 2D CAD design of the transducer.

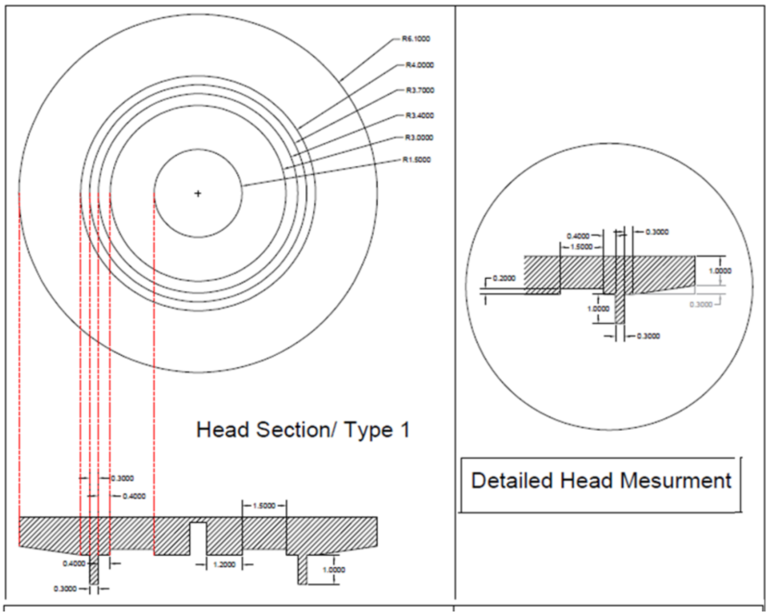

Figure 9: 2D CAD drawings for fabrication of the transducer head.

4.2 Transducer Simulation in Environmental (Water) Conditions

This section provides detailed modeling and simulation results of the ultrasonic transducer operating in a water environment under a pressure equivalent to a depth of 80 m below sea level.

Fig. 10 illustrates the acoustic pressure field and electrical potential distribution of the pinger system in water at a frequency of 11 kHz.

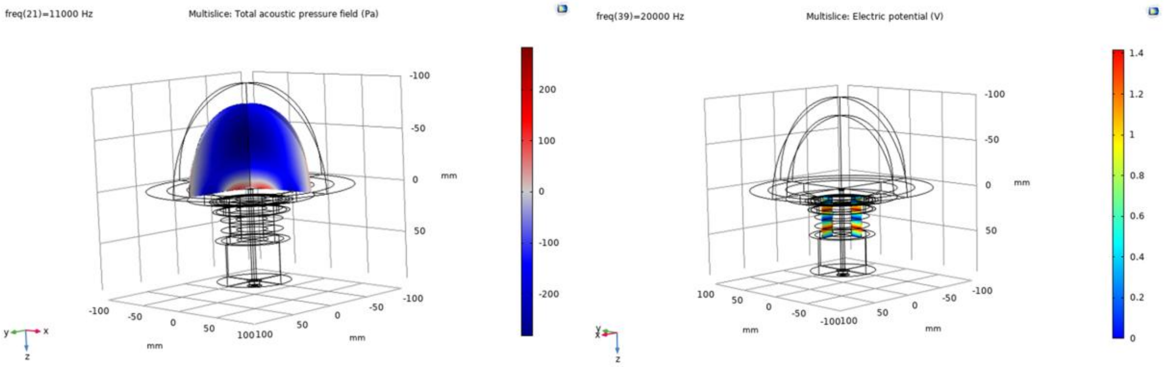

Figure 10: Pinger system in water, (left) acoustic pressure distribution, (right) electrical potential.

Fig. 11 presents the acoustic propagation pattern and the sound pressure level (SPL) distribution of the pinger system in water.

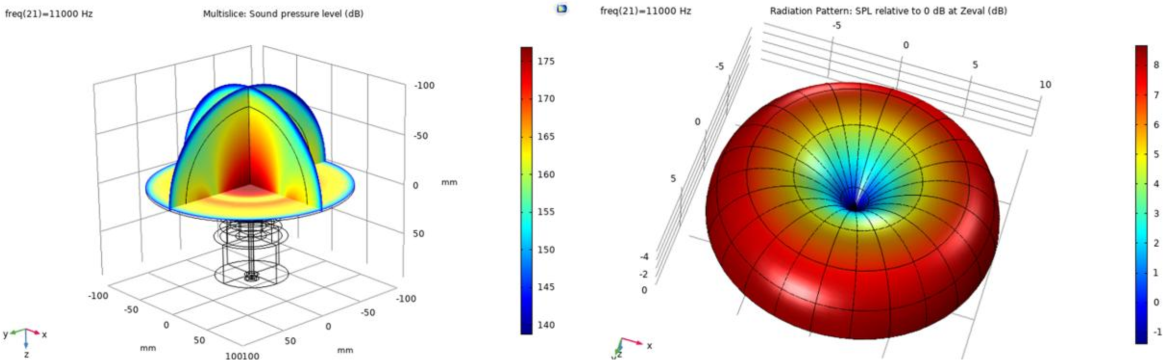

Figure 11: Pinger system in water, (left) acoustic propagation, (right) SPL distribution.

Fig. 12 shows a segment of the external SPL pressure field and the pressure–distance (z) plot under water conditions.

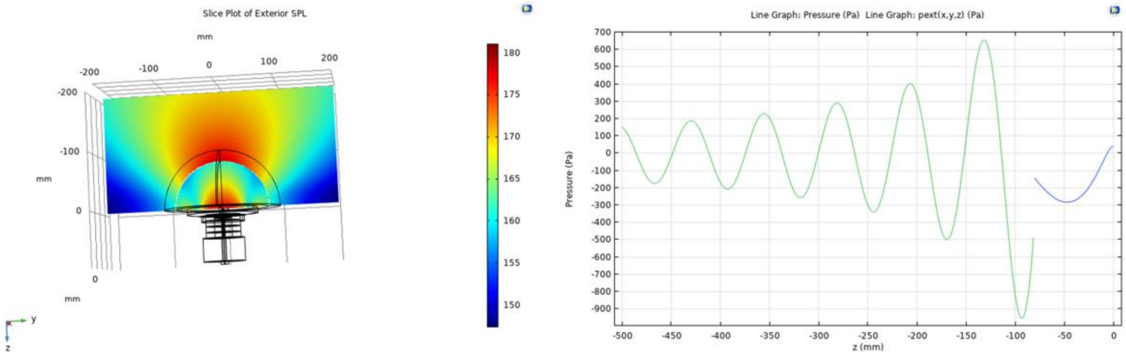

Figure 12: (left) portion of external SPL pressure field, (right) pressure vs. distance (z) graph.

Fig. 13 presents the admittance curve and power–frequency response of the pinger system in a water environment.

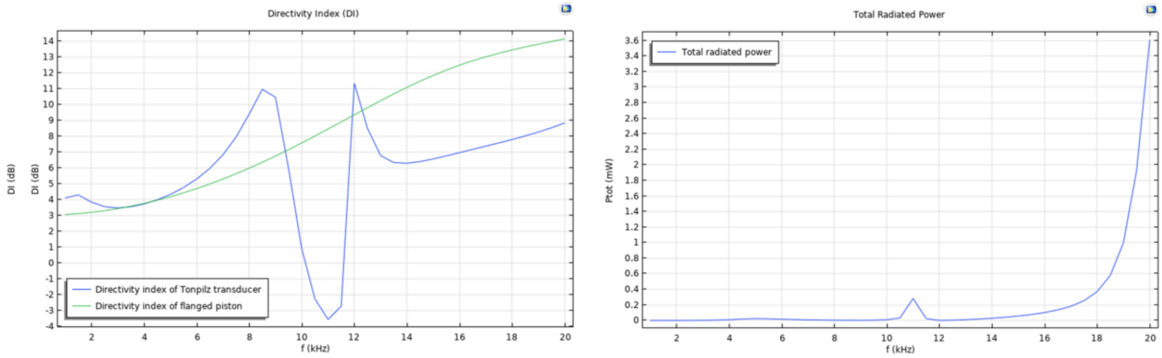

Figure 13: Pinger system in water — (left) admittance curve, (right) power–frequency response.

Fig. 14 displays the TVR curve and acoustic impedance of the pinger system in water.

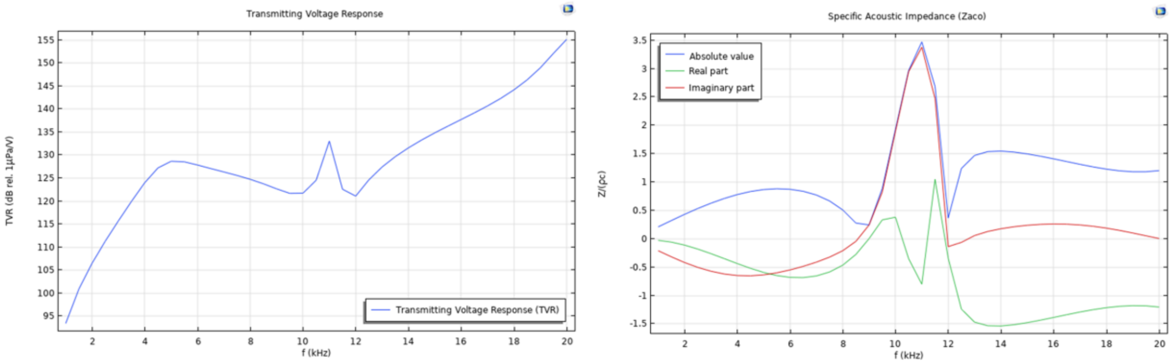

Figure 14: Pinger system in water — (left) TVR plot, (right) acoustic impedance.

The beam pattern obtained at 11 kHz is shown in Fig. 15, illustrating the acoustic wave propagation and beam angle of the Tonpilz-type transducer in the water medium.

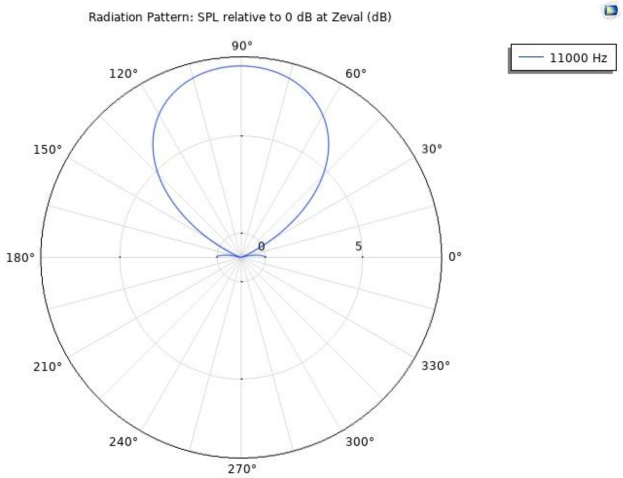

Figure 15: Beam pattern of the transducer at 11 kHz.

Finally, Fig. 16 presents the complete Tonpilz transducer model, including the piezoceramic, head, tail, housing, bolt, and the detailed housing dimensions.

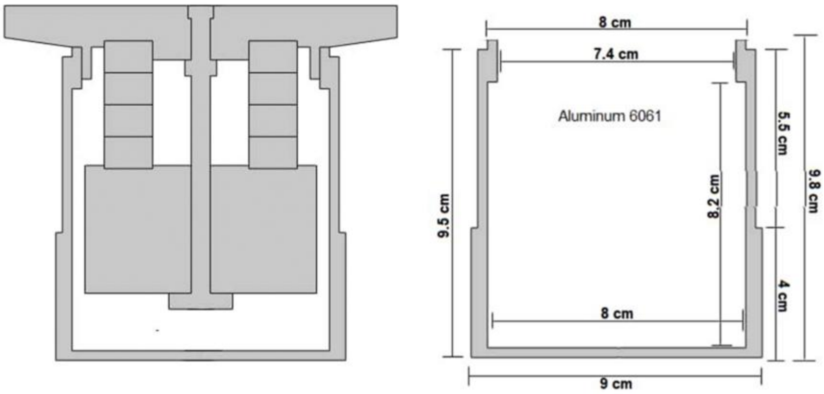

Figure 16: (left) final Tonpilz transducer model; (right) 2D view of the housing.

5. Construction of the Tonpilz Transducer

After completing the simulations and tuning the operating frequency to approximately 11 kHz, the fabrication of the Tonpilz transducer was carried out. This section describes the main components of the system, including the head, tail, housing, PZT-4 piezoceramic elements, and the tightening bolt, followed by an overview of the assembly and testing process.

5.1 Fabrication

Upon completion of the simulation stage and selection of the optimal structure and materials, the fabrication process of the Tonpilz transducer commenced. Fig. 16 illustrates the various components of the pinger together with its electronic driving circuit. Four PZT-4 piezoceramic rings, separated by copper electrodes, were bonded together using a high-strength adhesive. The positive poles were connected to each other, as were the negative poles. The piezoceramic stack was then clamped between the head and tail components using a stainless steel 316 bolt, tightened to a specific torque using a torque wrench. The applied torque directly affects the resonance frequency of the transducer.

Next, a polyurethane washer was placed around the tail section to improve longitudinal vibration and prevent bending of the bolt. Initial measurements were conducted using an impedance analyzer, function/signal generator, power amplifier, and oscilloscope. After optimizing the torque level, the housing was installed and sealed to ensure full waterproofing of the device. For better acoustic coupling and performance, castor oil was used to fill the interior of the housing.

Finally, the transducer was tested using Brüel & Kjær reference hydrophones, Types 8104 and 8105, to verify its acoustic response. Once satisfactory performance was achieved, the electronic driving and control circuit was designed, and the complete system underwent a final series of tests.

Figure 16: Components of the pinger along with the electronic circuit.

6. Conclusion

Tonpilz-type transducers play a crucial role in the design and development of fundamental sonar systems. In this study, by introducing slight modifications to the transducer's structure, the physical and environmental parameters such as water salinity, temperature, sound velocity, and material composition were modeled and optimized. The tail mass and bolt were fabricated from stainless steel 316, while the head and housing were made of aluminum alloy 6061.

Based on the simulation and experimental results, the constructed transducer using PZT-4 piezoceramic elements exhibited an optimal performance with a central frequency of approximately 11 kHz. When integrated with a water pressure sensor, this pinger can be employed as an underwater warning pinger (locator) for underwater safety and detection applications.

REFERENCES

1. X. Lurton, G. Lamarche, C. Brown, V. Lucieer, G. RIce, A. Schimel, & T. Weber, "Backscatter measurements by seafloor-mapping sonars", *Guidelines and recommendations*, *200*, (2015).
2. F. Campagnaro, F. Steinmetz, & B. C. Renner, "Survey on low-cost underwater sensor networks: From niche applications to everyday use", *Journal of marine science and*

engineering, *11*(1), 125, (2023).

3. R. Ghaffarivardavagh, S. S. Afzal, O.R. odriguez, & F. Adib, "Underwater backscatter localization: Toward a battery-free underwater GPS", In *Proceedings of the 19th ACM Workshop on Hot Topics in Networks* (pp. 125-131), (2020).
4. C. Wang, P. Du, Z. Wang, & Z. Wang, , "An Underwater Acoustic Network Positioning Method Based on Spatial-Temporal Self-Calibration", *Sensors*, *22*(15), 5571, (2022).
5. G. Cario, A. Casavola, G. Gagliardi, M. Lupia, & U. Severino, "Accurate localization in acoustic underwater localization systems", *Sensors*, *21*(3), 762, (2021).
6. E. Dubrovinskaya, P. Casari, & R. Diamant, "Bathymetry-aided underwater acoustic localization using a single passive receiver", *The Journal of the Acoustical Society of America*, *146*(6), 4774-4789, (2019).
7. M. Mirzaei Hotkani, J.F. Bousquet, S.A. Seyedin, , B. Martin, and E. Malekshahi, "Underwater target localization using opportunistic ship noise recorded on a compact hydrophone array", In *Acoustics* (Vol. 3, No. 4, pp. 611-629). MDPI, , (2021).
8. C. Alexandris, P. Papageorgas, & D. Piromalis, "Positioning systems for unmanned underwater vehicles: A comprehensive review", *Applied Sciences*, *14*(21), 9671, (2024).
9. T. Zhang, L. Chen, & Y. Li, "AUV underwater positioning algorithm based on interactive assistance of SINS and LBL", *Sensors*, *16*(1), 42, (2015).
10. H. Tang, H. He, F. Li, & J. Xu, "Underwater inertial error rectification with limited acoustic observations", *Satellite Navigation*, *5*(1), 3, (2024).
11. K. Listewnik, "Hydroacoustic multi-sensor for positioning underwater robots", *Solid State Phenomena*, *180*, 145-151, (2012).
12. N. R. Rypkema, H. Schmidt, & E. M. Fischell, "Synchronous-clock range-angle relative acoustic navigation: A unified approach to multi-AUV localization, command, control, and coordination", *Field Robotics*, *2*, 774-806, (2022).
13. A. Sánchez, S. Blanc, P. Yuste, A. Perles, & J. J. Serrano, "An ultra-low power and flexible acoustic modem design to develop energy-efficient underwater sensor networks", *Sensors*, *12*(6), 6837-6856, (2012).
14. N. Saeed, A. Celik, T. Y. Al-Naffouri, M. S Alouini, "Energy harvesting hybrid acoustic-optical underwater wireless sensor networks localization" *Sensors*, 18(1), 51, (2018).
15. I. F.Akyildiz, , D. Pompili, & T. Melodia, "Challenges for efficient communication in underwater acoustic sensor networks", *ACM Sigbed Review*, *1*(2), 3-8, (2004).
16. R. Matheson, "A battery-free sensor for underwater exploration", (2019).
17. J. Jang, & F. Adib, "Underwater backscatter networking", In *Proceedings of the ACM special interest group on data communication* (pp. 187-199), (2019).
18. Z. Yang, L. Ma, R. Zhang, J. Zhang, F. Liu, & X. Xiao, "Acoustic Energy Harvested Wireless Sensing for Aquaculture Monitoring", *Inventions*, *10*(3), 41, (2025).
19. J. Y. Pyun, Y. H. Kim, & K. K. Park, "Design of piezoelectric acoustic transducers for underwater applications", *Sensors*, *23*(4), 1821, (2023).
20. A. G. Every, R. E. Vines, and J. P. Wolfe. "Line-focus probe excitation of Scholte acoustic waves at the liquid-loaded surfaces of periodic structures", *Physical Review* B 60, no. 16: 11755, (1999).
21. J. Jang, & F. Adib, "Underwater backscatter networking", In *Proceedings of the ACM special interest group on data communication* (pp. 187-199), (2019).
22. N. Saeed, A. Celik, T. Y. Al-Naffouri, & M. S. Alouini, "Energy harvesting hybrid acoustic-optical underwater wireless sensor networks localization", *Sensors, 18*(1), 51, (2017).

23. S. M. Kargar, & G. Hao, "An atlas of piezoelectric energy harvesters in oceanic applications", *Sensors*, *22*(5), 1949, (2022).
24. P. Oppermann, & B. C. Renner, "Low-Power Underwater Acoustic Tracers for Long-Range River Bedload Monitoring", *Proceedings of the 18th International Conference on Underwater Networks & Systems* (pp. 1-8), (2024).
25. R. Fu, X. Zhang, C. H. Yu, K. Liu, T. Haque, L. Ouyang, & M. M. C. Cheng, "A Thin Flexible Acoustic Transducer with piezoelectric-actuated microdomes for Underwater Communication", *arXiv preprint arXiv:2504.16212*, (2025).
26. L. Schulthess, P. Mayer, L. Benini, & M. Magno, "A passive and asynchronous wake-up receiver for acoustic underwater communication", *International Symposium on Power Electronics, Electrical Drives, Automation and Motion (SPEEDAM)* (pp. 480-485). IEEE, (2024).
27. E. K. Skarsoulis, G. Piperakis, M. Kalogerakis, E. Orfanakis, P. Papadakis, S. E. Dosso, & A. Frantzis, "Underwater acoustic pulsed source localization with a pair of hydrophones", *Remote Sensing*, *10*(6), 883, (2018).
28. S. A. Swift, & A. S. Bower, "Formation and circulation of dense water in the Persian/Arabian Gulf", *Journal of Geophysical Research: Oceans*, *108*(C1), 4-1, (2003).
29. I. Sinclair, (2000). *Sensors and transducers*. Elsevier.
30. https://www.google.com/url?sa=t&source=web&rct=j&opi=89978449&url=https://www.comsol.jp/paper/download/84155 vadde_paper.pdf&ved=2ahUKEwjEm8bd6umQAxVCif0HHZeeKnMQn5YKegQIERAB&usg=AOvVaw1Zk5PxMn6cCfky0hTXdfR_
31. https://www.comsol.jp/paper/download/84155/vadde_paper.pdf&ved=2ahUKEwib38HG8emQAxXqVKQEHTgUFhUQ6vUJegQIIhAA&usg=AOvVaw1Zk5PxMn6cCfky0hTXdfR_
32. S. C. Butler, "A 2.5 kHz magnetostrictive tonpilz sonar transducer design", *The Journal of the Acoustical Society of America*, *109*(5_Supplement), 2459-2459, (2001).
33. Y. Roh, & X. Lu, "Design of an underwater Tonpilz transducer with 2-2 mode piezocomposite materials", *The Journal of the Acoustical Society of America*, *119*(6), 3734-3740, (2006).